

ROCK FRAGMENTATION BY HIGH FREQUENCY FATIGUE

FRAGMENTATION D'UNE ROCHE PAR FATIGUE À HAUTE FRÉQUENCE

HOCHFREQUENZ DURCH FELSDAUERSCHWINGZERBRECHUNG

Patrick J. CAIN

Syd S. PENG

Egons R. PODNIEKS

Twin Cities Mining Research Center, Bureau of Mines
Twin Cities, Minnesota

SUMMARY

The fatigue failure characteristics under high frequency (10 KHz) cyclic loading were determined for Tennessee marble, Charcoal granite, and Sioux Quartzite. The fatigue strength for each rock type shows a correlation with the static strength. The analysis of the damping and internal heat generation indicated that nearly all of the power input was accounted for as a change in enthalpy. The thermal strain was calculated and found to range up to 30 pct of the dynamic strain amplitude. The specific energy required for failure was determined and possible applications are discussed.

SOMMAIRE

Les caractéristiques de la rupture du marbre du Tennessee, du granite dit 'Charcoal' et du quartzite 'Sioux' ont été déterminées par des essais de fatigue à haute fréquence (10 kHz). Une corrélation existe entre la limite d'endurance et la résistance statique. L'analyse de l'amortissement et de la production de chaleur indique que la plus grande partie de la puissance absorbée est retrouvée comme un changement en enthalpie. Le calcul de la déformation thermique démontre que celle-ci peut monter jusqu'à 30 pour cent de l'amplitude des déformations dynamiques. Nous avons déterminé l'énergie spécifique nécessaire pour causer la rupture, et présenté des applications potentielles.

ZUSAMMENFASSUNG

Die Eigenschaften der Dauerschwingzerbrechung des 'Tennessee' Marmors, des 'Charcoal' Granites und des 'Sioux' Quarzites wurden unter Hochfrequenz (10 kHz) gemessen mittels Dauerfestigkeitsproben mit periodischer Belastung. Die Dauerfestigkeit steht in Wechselbeziehung zur statischen Festigkeit. Die Analyse der Dämpfung zeigt, dass der grösste Anteil der zugeführten Energie in einer Enthalpie-änderung verbraucht wird. Die Kalkulation der Wärmedehnung zeigt, dass diese bis zu 30 Prozent der gesamten Dehnungsamplitude reichen kann. Die spezifische Energieforderung zur Zerbrechung ist bestimmt worden, und mögliche Anwendungen werden diskutiert.

INTRODUCTION

The effect of low-frequency cyclic loading on rock is an area which has been investigated to a limited extent (Burdine, 1963; Haimson, 1972; Haimson, 1973; Peng, 1973). Also acoustic methods have been used to determine the physical and structural properties of rock. Ultrasonic devices have been frequently mentioned in discussions of novel rock fragmentation techniques (Farmer, 1965; Maurer, 1970). Past efforts to use sonic devices as cutting tools have employed a transducer driving a cutting medium such as an abrasive slurry (Goetze, 1956) or a bouncing tool (Graff, 1971). As the energy available from sonic transducers has increased, it is now important to explore the possibility of fracturing rock by sonic energy. In this program a failure of rock by the direct application of sonic energy is being investigated.

The energy required to maintain the vibrations and induce failure is primarily determined by the damping or energy dissipation. In this investigation the energy dissipation or internal friction has been used to predict the heating and the resulting thermal

stresses which may influence the fracture of the specimens.

EXPERIMENTAL PROCEDURE

Three rock types, Charcoal granite, Tennessee marble, and Sioux Quartzite, were chosen to provide specimens with different ductilities and static strengths. The properties of these rocks are listed in Table 1.

The power source used in these experiments was a piezoelectric transducer connected to the cylindrical rock specimens by a transmission line as shown in Figure 1. The transducer is a high Q resonant device with a catenoidal horn for amplification and a nominal resonant frequency of 10,150 Hz. The complete system carries two standing waves and each component has free ends and the connections are only lightly stressed. This arrangement is advantageous because the maximum strain is at the center of the specimen and the end effects are negligible.

TABLE 1. - Mechanical and thermal properties of Charcoal granite, Tennessee marble, and Sioux Quartzite

| Properties | Charcoal granite | Tennessee marble | Sioux Quartzite |
|---|-----------------------|-----------------------|---------------------|
| Uniaxial compressive strength..... $\frac{\text{kN}}{\text{m}^2}$ | 2.30×10^5 | 1.16×10^5 | 3.89×10^5 |
| Uniaxial tensile strength..... $\frac{\text{kN}}{\text{m}^2}$ | 1.22×10^4 | 8.40×10^3 | 1.83×10^4 |
| Young's modulus, E..... $\frac{\text{kN}}{\text{m}^2}$ | 6.76×10^7 | 6.20×10^7 | 6.96×10^7 |
| Thermal diffusivity, α $\frac{\text{cm}^2}{\text{sec}}$ | 9×10^{-3} | 10.7×10^{-3} | 20×10^{-3} |
| Thermal conductivity, k..... $\frac{\text{cal}}{\text{cm sec } ^\circ\text{C}}$ | 5.17×10^{-3} | 6.6×10^{-3} | 12×10^{-3} |
| Thermal expansion coefficient, α^* $\frac{1}{^\circ\text{C}}$ | 10×10^{-6} | 10×10^{-6} | 15×10^{-6} |

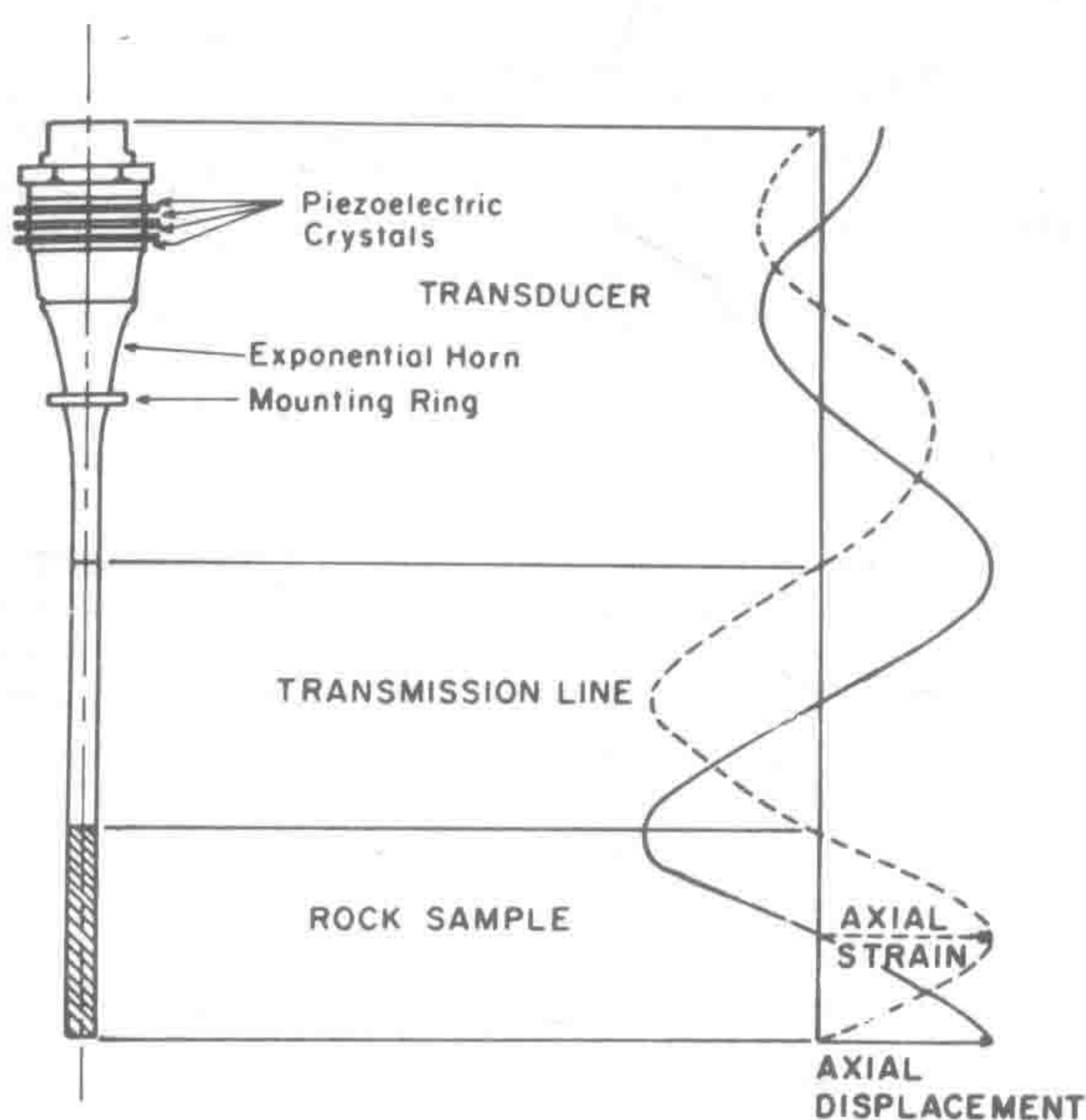


FIGURE 1. - Transducer-Specimen Assembly With Strain and Displacement Mode Shapes.

The rock specimens were cylinders 1 inch in diameter and 10 inches long. In preparing specimens for testing, a pair of strain gages were bonded on opposite sides of the midpoint of the specimen and wired in opposite sides of a wheatstone bridge to indicate axial strain. The resonant frequency of the specimen was matched to that of the transducer by trimming the ends of the specimen. To provide an indicator of specimen structural condition before and after testing, the longitudinal pulse travel velocity was determined.

The input power was provided by a 200-watt power amplifier controlled by a variable-frequency

oscillator. The input voltage, input current, and strain amplitudes were monitored. The strain amplitude was recorded on a strip chart together with the temperature at the strain gage location.

During each test the input frequency was regulated to maintain resonance in the system, and the voltage was regulated to maintain constant strain amplitude in the rock specimen. The maximizing of the strain amplitude was used as the criterion for resonance. The fatigue tests were terminated when pronounced detuning or irregular input current and strain gage signals were observed. In some cases the rock specimen was broken in several parts at failure. If the specimen did not fail, the test was terminated after approximately 10^8 cycles were reached.

Postfailure testing included measuring the bar resonant frequency of intact specimens and the longitudinal ultrasonic pulse travel time. The specimens were cut in half lengthwise, and the cut surfaces were ground and polished so the extent of the fatigue cracks could be determined.

In addition to the fatigue test specimens, one specimen of each rock type was tested at amplitudes increasing in steps so that the rate of temperature increase as a function of amplitude could be determined for a single specimen.

EXPERIMENTAL RESULTS

The data taken in the course of the experiments included the number of cycles to failure as a function of the strain amplitude and the temperature of the specimen as a function of time. The relationship between strain amplitude and the number of cycles to failure for Charcoal granite, Tennessee marble, and Sioux Quartzite is shown in Figure 2. The strain amplitudes at failure are small, but it must be noted that rock fails in tension at low strains. The sonic strain amplitudes at failure are a significant fraction of the quasi-static tension failure strain (15-50 pct). However, on the compressive side of the load cycle, the strain amplitude is very small (less than 5 pct) compared with the strain at quasi-static compressive failure.

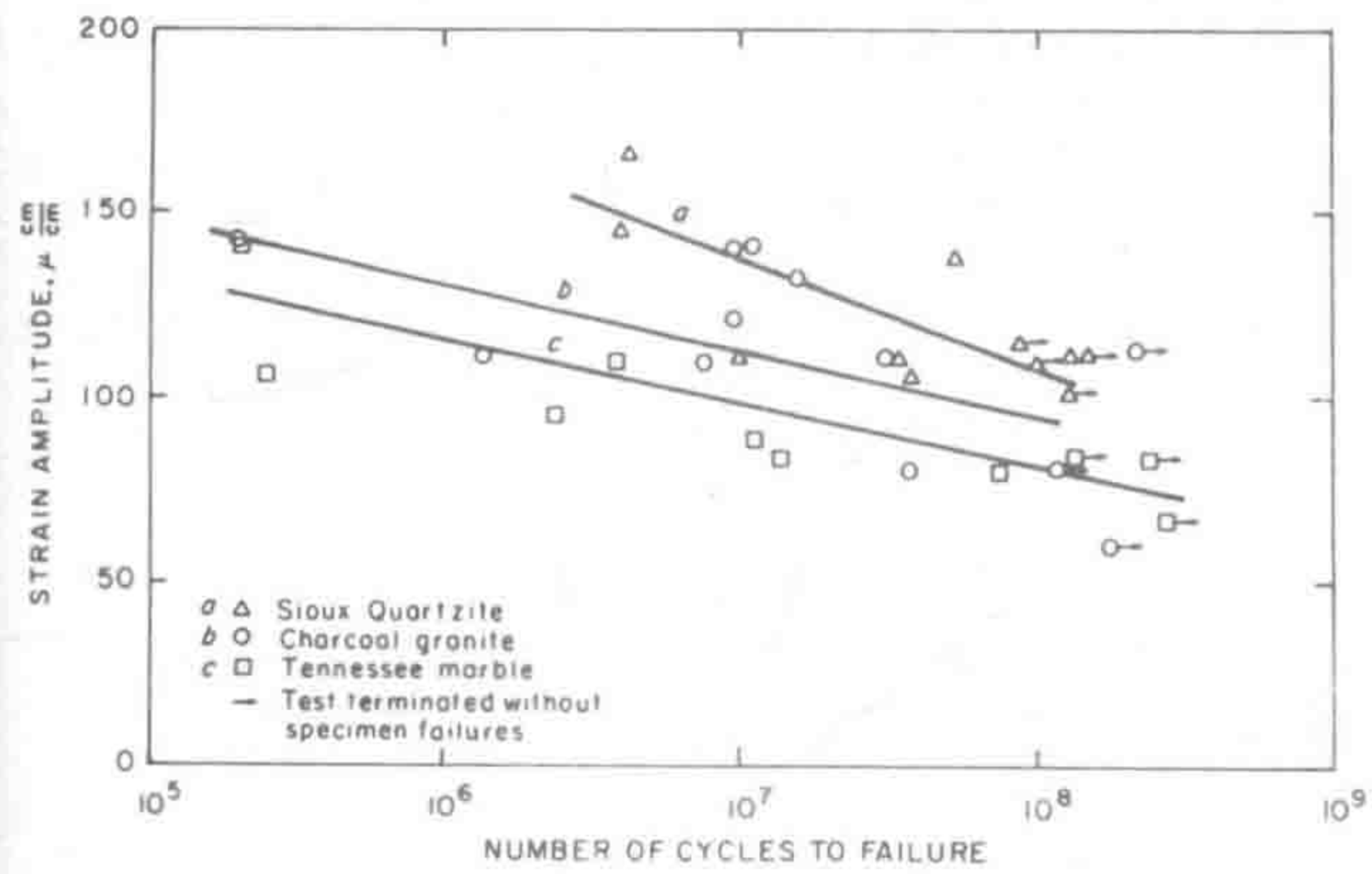


FIGURE 2. - Variation of Fatigue Life With Strain Amplitude for Tennessee Marble, Charcoal Granite, and Sioux Quartzite.

The three rock types tested had similar exponential relationships between the number of cycles to failure and the strain amplitude (fig. 2). The endurance limit is related to the static tensile strength, with the rock type with the highest strength, Sioux Quartzite, requiring the greatest number of cycles to failure and that with the lowest strength, Tennessee marble, requiring the least number at a given strain amplitude.

Close examination of the cracks revealed a fractured zone of less than individual grain size on either side of the crack in all three rock types. These zones were composed of small branching cracks on the planes of maximum shear at 45 degrees to the crack line. Formation of single large cracks normal to the specimen axis indicates the failure is primarily tensile. The distribution of the fracture locations in the maximum strain region indicates that fracture location depends on weak points in the rock. Both intergranular and transgranular cracking occurred in each sample.

A typical time history of the surface temperature at the center of a Charcoal granite specimen is shown in Figure 3. When loading begins at time $t = 0$ the temperature increases rapidly and almost linearly to point a, then continues to increase at a decreasing rate to point b, where it begins to approach asymptotically a steady state which is maintained until failure. Many specimens failed before steady state temperature conditions were reached. The maximum temperatures ranged up to 160°C depending on the strain amplitude and rock type. The highest temperatures were usually observed in tests of Sioux Quartzite.

The initial constant rate of temperature increase is proportional to the energy being dissipated in the specimen. The rate of temperature increase as a function of strain amplitude for single specimens of each rock type is shown in figure 4. Using single specimens reduces scatter caused by material variations and emphasizes the relationship with strain amplitude. The rate of temperature increase is approximately proportional to the cube of strain amplitude.

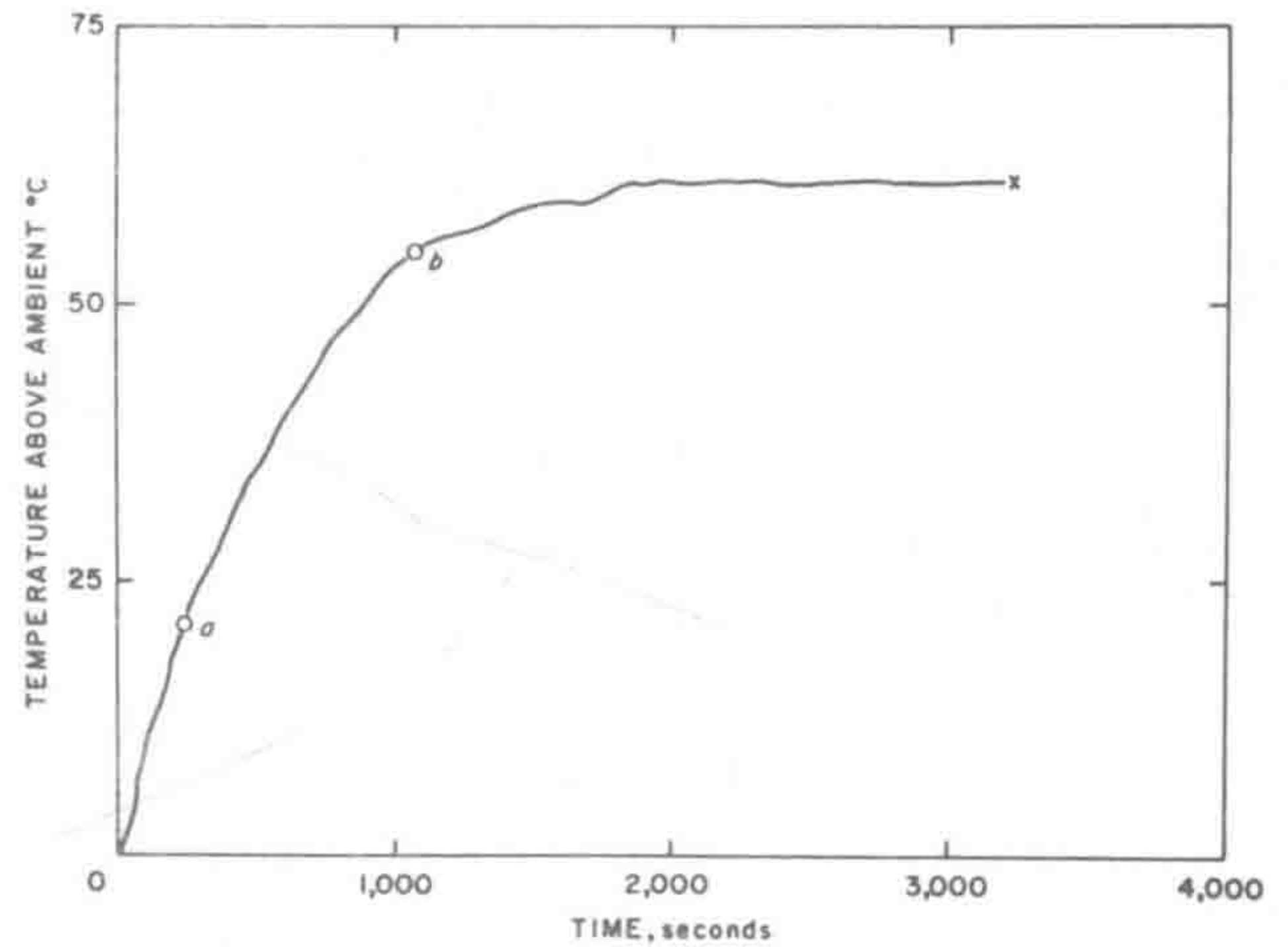


FIGURE 3. - Surface Temperature Increase Above Ambient for a Charcoal Granite Specimen With a Strain Amplitude of $140 \mu \text{ cm/cm}$.

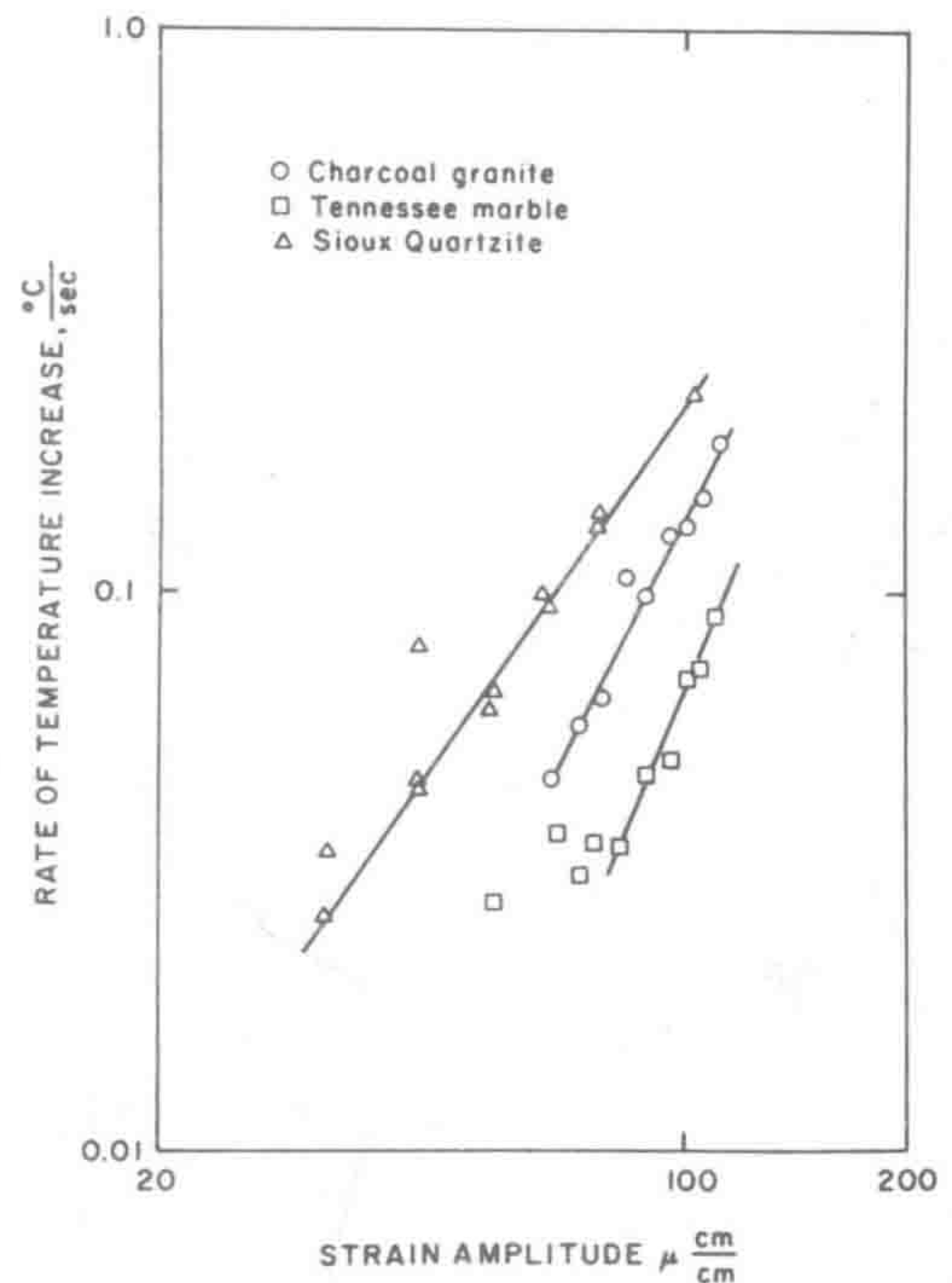


FIGURE 4. - Initial Rates of Temperature Increase for Various Strain Amplitudes.

The internal heat generation in the specimen can be expressed in terms of heat balance in midsection of the specimen during the initial loading. When the temperature is low and no heat is being lost at the boundary, the rate of internal heat generation equals the product of the rate of temperature increase, T , and the heat capacity of the material:

$$g = Tc\rho \quad (1)$$

where c is the specific heat and ρ is the density.

In a material property approach (Lazan, 1964) the energy dissipation per unit volume during each cycle is assumed to have a power law dependence on strain ϵ_o ; therefore the rate of heat generation g at the specimen midsection is

$$g = d\epsilon_o^n f \quad (2)$$

where f is the loading frequency. It has been assumed that all dissipated energy is in the form of heat. Combining the damping relation (2) with the thermodynamics equation (1) gives

$$\frac{dT}{dt} = \frac{d\epsilon_o^n f}{\rho c} \quad (3)$$

From the experimental data (Figure 4) the exponent can be evaluated as $n = 3$ and if it is assumed that the same relationship holds for the entire volume of the specimen, then the distribution of internal heating, G , is

$$G = df\epsilon_o^3 \sin^3 \frac{\pi Z}{L} \quad (4)$$

where L is the length of the specimen and Z is the axial coordinate.

The power P or rate of energy input to the specimen must equal that dissipated in the specimen. From the sinusoidal strain distribution this is

$$P = \frac{4}{3} b^2 L g \quad (5)$$

where b is the radius of the specimen.

Using the theoretical internal heat generation rate, the temperature distribution in a solid cylinder with outer radius b and length L is calculated by the usual methods of heat transfer analysis (Ozsisik, 1968). In the calculation, the boundary heat transfer coefficients were estimated and the internal heat generation distribution was determined by equation 4. The theoretical temperature distribution predicted the measured temperatures with sufficient accuracy to validate the assumption that all input power was dissipated in the form of heat.

This temperature distribution is then used to calculate the thermal stress in the specimen (Timoshenko, 1951). The state of stress in the center section of the specimen can be approximated by plane strain conditions because of the long slender nature of the specimen. Equations for thermal stresses developed in the specimens were derived and used to determine the thermal stress values for the three rock types tested (Cain, 1974).

The cyclic strain is axial and the fractures are formed normal to the axis; thus, only the axial thermal strains affect fracture. The results showed that the axial thermal strain is compressive in the specimen center and tensile at the outer surface. The peak tensile stress which is the sum of the alternating strain amplitude and the thermal strain at the outer edge can be expected to control failure. To evaluate the contribution of the thermal strain to the peak tensile strain, the maximum tensile stress is shown as a function of time in Figure 5.

The specific energy for fatigue failure, E_v , is defined as the total energy input per unit volume to the specimen before failure and is a parameter used

to evaluate the fragmentation efficiency. In the case of the longitudinally resonating fatigue specimens the energy is not uniformly distributed due to the sinusoidal strain distribution. The maximum specific energy will be located at the specimen midsection where the fractures occurred. The rate of energy input to a unit volume at the midsection, g , can be found from equation 5. The specific energy at the midsection is

$$E_v = g \frac{N}{f} = \frac{P}{\frac{4}{3} b^2 L} \frac{N}{f} \quad (6)$$

where N is the number of cycles to failure. In this way the damping, which determines g , determines the energy consumed before failure.

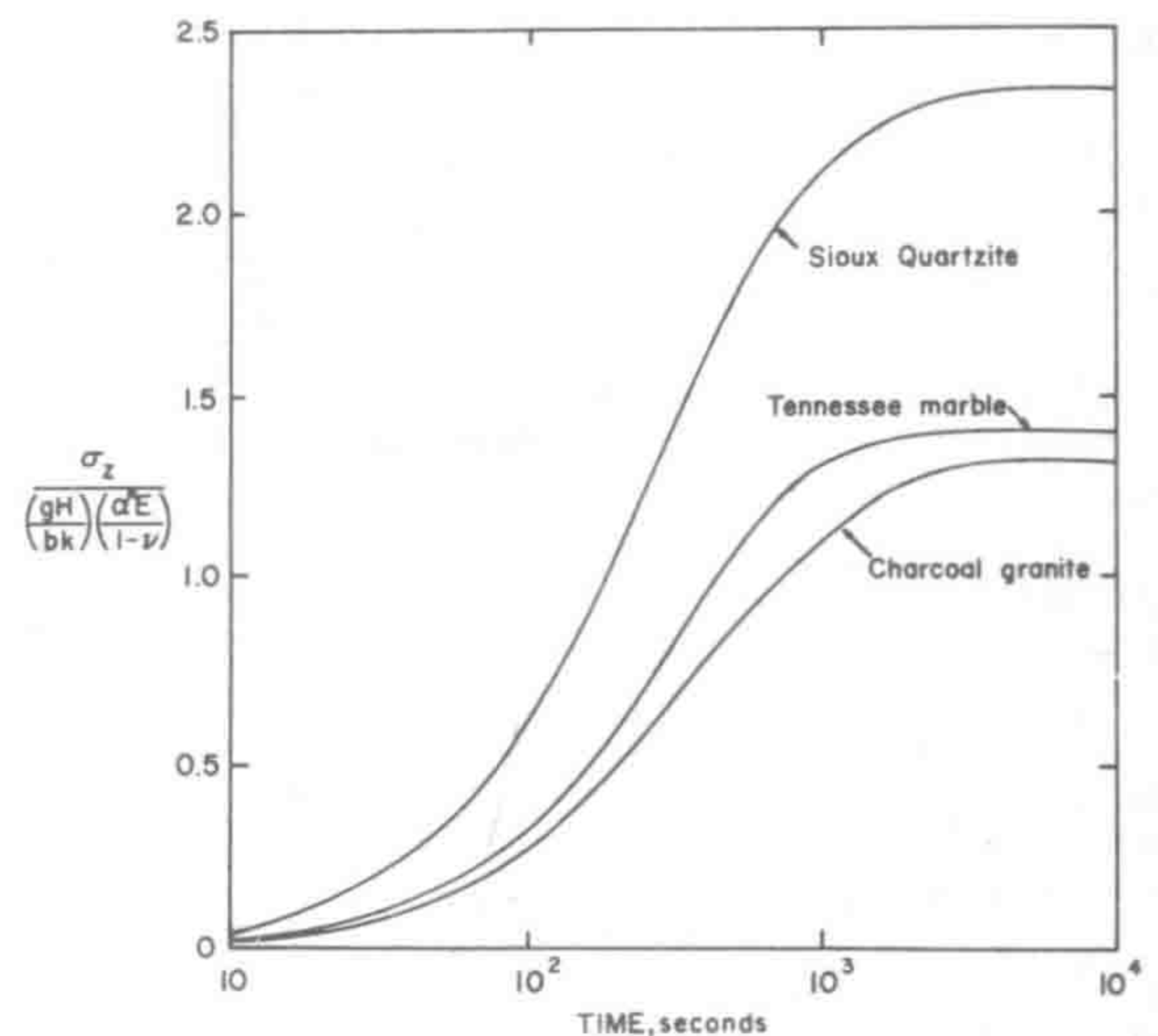


FIGURE 5. - Variation of Maximum Axial Tensile Thermal Stress With Time.

DISCUSSION OF THE RESULTS

The ratio of thermal to vibrational strain will increase with time because the thermal strain increases while the vibrational strain amplitude is constant. The dependence of the ratio on the strain amplitude is controlled by two opposing trends. Increasing the strain amplitude rapidly decreases the number of cycles, or time, before failure while increasing the heating rate and equilibrium temperature.

These two effects combine so that for extremely high and low strain amplitudes the thermal strains are small. The peak thermal strains experienced by any rock type are on the order of 30 pct; although this is not large enough to cause fracture, it is too large to neglect and must be considered as a contributing factor.

The specific energy, E_v , requirements are shown as a function of the number of cycles to failure in Figure 6. The dominant factor in determining the specific energy is the number of loading cycles. From

Figure 2, the change of strain amplitude is quite small compared with the change in the number of cycles to failure. At first it appears that the most efficient process from specific energy considerations is to fracture the rock with the least number of loading cycles. However, the principal advantage of a vibratory or oscillatory load is that it can form tensile fractures, which requires lower stresses than compressive fractures.

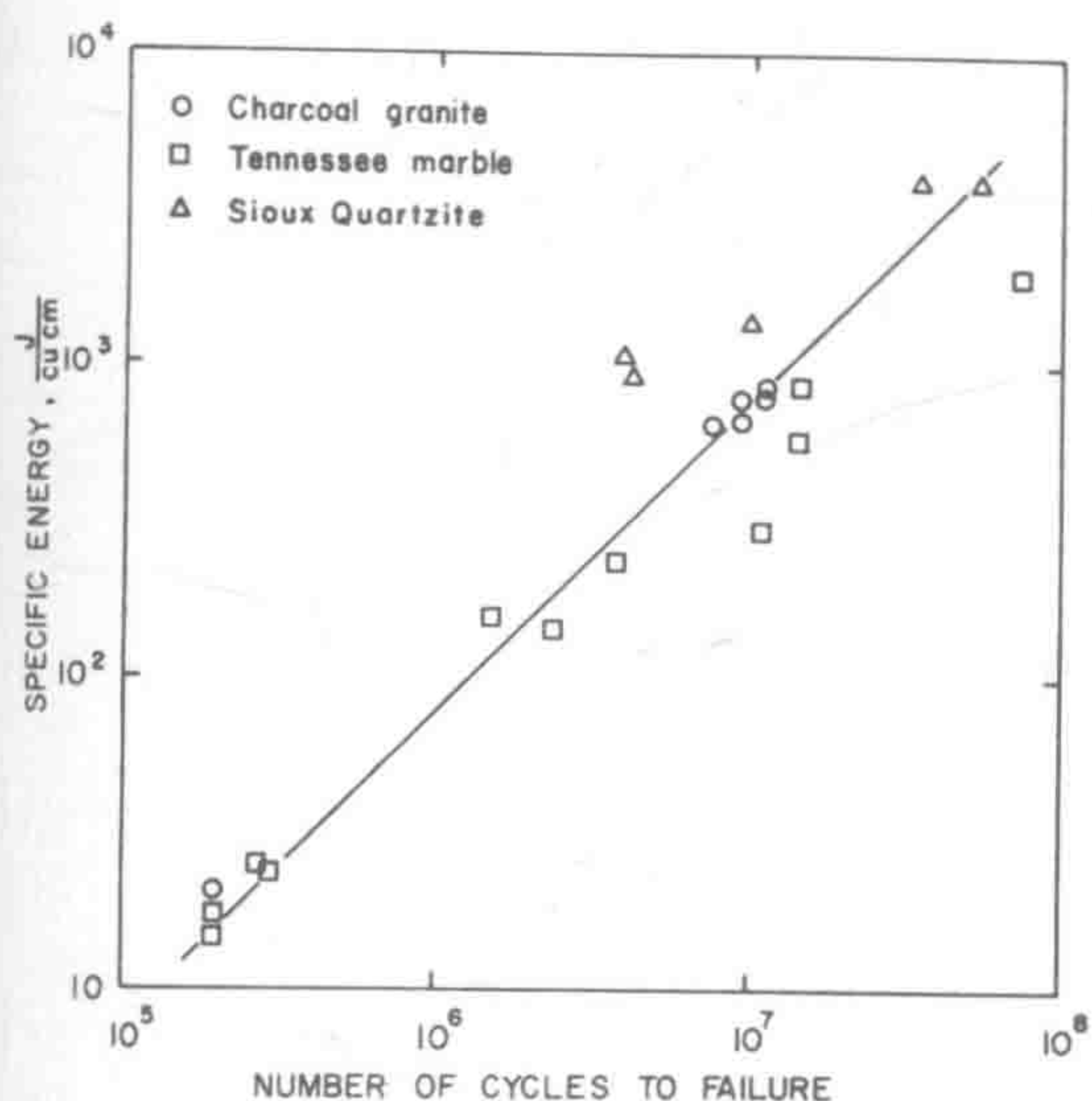


FIGURE 6. - Variation of Specific Energy With the Number of Cycles to Failure for Fatigue Fracture.

An important point of interest is the comparison of fatigue failure of rock under high (10 KHz) and low (1-4 Hz) frequency loading. Since different rock types have been investigated, the tests must be compared on the basis of the ratio of the applied stress to the static strength. By this method the effect of tensile and compressive loading can be compared. Peng (1973) and Haimson (1973) also tested rock under alternating tension-compression loading and reported that rock could be fatigue fractured with peak tensile loads as low as 40 pct of the tensile strength. Although in both cases the amplitude of the compressive portion of the load cycles exceeded the tensile by a factor of approximately 10, the tensile load amplitudes are similar to the tensile and compression load amplitudes used in this work. The results in terms of fatigue limit for both high-frequency and low-frequency alternating compression-tension tests are similar except that rock could be fragmented by load amplitudes as low as 30 pct of the static strength with the high-frequency loading. The important point is that the fatigue failure is reached in much less time with high-frequency loading. The fractures produced by both high- and low-frequency alternating tension-compression loading were of tensile nature. The heating effects were not observed in low-frequency fatigue (Haimson, 1973) because at the low rates (1-4 Hz) any heat generated by internal friction can readily dissipate.

In evaluating the potential application of high-frequency fragmentation methods, there are two modes to consider, i.e., breaking rock from the free face of a semi-infinite rock mass, or fragmenting rock with finite dimensions. The criterion to be used for such an evaluation is the comparison of the energy consumption and wear of the tools and equipment. If a vibratory tool is acting on a free rock face of a semi-infinite body and the mechanical impedance of the device and the face is matched, the stress waves can be transmitted into the body. However, if the impedance is mismatched, energy transfer will be inefficient and high interface stresses will be generated. To meet the goal of low tool wear, an impedance-matched system is necessary. The problem of energy being carried from the face into the rock mass by stress waves decreases with higher frequency vibrations, since the vibrations are rapidly attenuated by damping and the input energy will remain near the face in the form of thermal or strain energy. The energy losses can be minimized further if the amplitude is sufficiently high to cause failure in a short time. This does not necessarily imply that a single-cycle static loading is optimum, because the advantage of achieving tensile fracture (through dynamic loading) would then be lost.

On the other hand, in a rock mass of finite dimensions the stress waves are contained within the body and if the loading frequency is matched to the natural frequency, determined by the rock properties and dimensions, a resonant state of vibration can be achieved. When the high-frequency loading is applied in this manner, large amplitudes can be built up with a minimum of stress on the interface between the tool and the rock. This concept can be used to design a crusher to handle very hard rocks.

CONCLUSIONS

1. The endurance in high-frequency fatigue was related to tensile strength; rocks with higher static tensile strengths require more load cycles to be fractured at a given load amplitude.
2. Rock can be fatigue-fractured by high-frequency load amplitudes as low as 30 pct of the static tensile strength.
3. The fractures observed under high-frequency alternating tension-compression loading were tensile in nature.
4. Nearly all of the energy transferred to the specimen was accounted for as heat generated in the specimen.
5. For the rocks tested it was observed that, based on energy consideration, the most efficient cyclic fragmentation method is that requiring the least number of loading cycles to fragment rock at resonance.
6. At this time it appears the most promising immediate application of high-frequency fatigue will be in the fragmentation of large pieces of hard rock.

REFERENCES

- Burdine, N. T. Rock Failure Under Dynamic Loading Conditions. Journal of Soc. of Petroleum Engr., March 1963, pp. 1-8.
- Cain, P. J. Private Communication, 1974. Available on request from R. A. Friedel, Bureau of Mines, Minneapolis, Minn.
- Farmer, I. W. New Methods of Fracturing Rocks. Mining and Minerals Engineering, January 1965, pp. 177-184.
- Goetze, D., and G. E. Miller. An Investigation of the Ultrasonic Disintegration of Solids. WADC Tech. Rept. 55-277, June 1956.
- Graff, K., et al. Fundamental Studies in the Use of Sonic Power for Rock Cutting. Annual Technical Report, for ARPA Contract No. H0210010 monitored by U.S. Bureau of Mines, The Ohio State University Research Foundation, December 1971, pp. 18-27.
- Haimson, B. C. Mechanical Behavior of Rock Under Cyclic Loading. Annual Report for ARPA Contract No. H0210004 monitored by U.S. Bureau of Mines, the University of Wisconsin, Madison, Wis., March 1972, p. 92.
- Haimson, B. C. Mechanical Behavior of Rock Under Cyclic Loading. Annual Report for ARPA Contract No. H0220041 monitored by U.S. Bureau of Mines, the University of Wisconsin, Madison, Wis., April 1973, p. 88.
- Lazan, B. J. Damping Studies in Materials Science and Materials Engineering. ASTM, STP 378, June 1964, pp. 1-20.
- Maurer, William C. Potential Application of Novel Rock Disintegration Techniques in Mining. 31st Annual Mining Symposium, Duluth, Minn., January 1970, p. 187.
- Ozsisik, M. N. Boundary Value Problems of Heat Conduction. Internat. Textbook Co., 1968, p. 150.
- Peng, S. S., E. R. Podnieks, and P. J. Cain. Study of Rock Behavior in Cyclic Loading. Presented at the 6th Conference on Drilling and Rock Mechanics at Austin, Tex., January 22-23, 1973, SPE preprint No. 4249, pp. 181-192.
- Timoshenko, S., and J. N. Goodier. Theory of Elasticity. McGraw-Hill Book Co., 2nd ed., 1951, p. 406.